ELSEVIER

Study of the Degree of Hydration of Concrete by Means of Image Analysis and Chemically Bound Water

M. Mouret, A. Bascoul, and G. Escadeillas
Laboratory of Materials and Durability of Constructions, INSA/UPS, Toulouse, France

This article deals with the effect of both initial temperature and subsequent high curing temperature on the degree of hydration of normal strength concrete at the age of 28 days. Variations in compressive strength were observed and presented previously. Here, their causes are investigated through a difference in the hydration state in relation with the initial mixing and curing conditions. We present two ways of measuring the degree of hydration and compare the results, first by means of an original technique of image analysis on flat polished sections observed by scanning electron microscope, and second by classical measurement of the chemically bound water. Two kinds of specimens are studied. Cylinders of 11 cm × 22 cm were prepared with two different temperature formulae of constituents: 20°C (water)—20°C (aggregate)—20°C (cement); and 20°C (water)—70°C (aggregates)—70°C (cement), so as to obtain an initial temperature of the mixes between 20°C and 50°C, respectively. Specimens were sealed and cured under either controlled laboratory conditions or simulated conditions of hot weather. In each case, all the specimens were stored in water up to 28 days.
ADVANCED CEMENT BASED MATERIALS 1997, 6, 109–115.

KEY WORDS: Chemically bound water, Degree of hydration, Image analysis

Drops in strengths are observed during summer on specimens for manufacturing control tested in the laboratory at 28 days, even if particular attention is given in order to avoid the well-known disorders that are induced by hot weather [1].

A previous study pointed out drops in 28-day compressive strength and 28-day splitting tensile strength of laboratory concrete performed with high initial temperature (approximately 50°C) and subjected to high curing temperature (35°C) [2]. An increase in the water demand could not fully explain the drops in compressive strength by applying Feret's rule. Consequently, it appeared necessary to study the hydration state of concrete in relation with both high initial and subsequent curing temperatures corresponding to our tests. Indeed, we cannot rely on the literature in order to link together temperature, strength, and degree of hydration. This issue gives rise to conflicting results [3–5].

For the last 10 years, various image analysis methods have been developed and used to characterize some features of cement based materials [6–12]. Direct observation of polished sections can be a very helpful tool to directly assess the degree of hydration, using image analysis technique from backscattered electron imaging (BSEI).

This article presents the method we developed in order to extract and count the remaining unhydrated cement grains at the age of 28 days. In addition, we give a comparison with the classical method of chemically bound water.

Experimental Program

Different temperature formulae of constituents were applied to two kinds of mixing so as to obtain two 28-day nominal strengths, 35 and 22 MPa. Manufacturing details are given in Table 1. Rounded siliceous aggregates were used with ordinary Portland cement (OPC). Concerning series D, plasticizer was incorporated by 0.3% per weight of cement. For the basic composition, the water/cement (w/c) ratios were 0.52 and 0.73 for series C and D, respectively.

For each series the same workability was imposed whatever the temperature (80-mm slump for series C, 90-mm slump for series D), because this parameter must be constant on building sites. Water was added for C2 and D2 (approximately 20 to 30 L/m^3 extra quantities of water as compared to references C1 and D1). This amount of added water was essentially needed to compensate for the evaporation, as it was verified by measuring the water actually contained (W_{ac}) in the mix. In this way, the actually W/C ratios deviated from the basic values of about 2% (series C)

Address correspondence to: Dr. M. Mouret, Laboratory of Materials and Durability of Constructions, INSA/UPS, Avenue de Ranguiel, 31077 Toulouse cedex, France.
Received June 6, 1996; Accepted August 14, 1997

ISSN 1065-7355/97/$17.00
PII S1065-7355(97)00033-3

TABLE 1 Manufacturing details

	Initial Temperature	Series C	Series D
20°C (water)—20°C (aggregate)—20°C (cement)	~20°C	C1	D1
20°C (water)—70°C (aggregate)—70°C (cement)	~50°C	C2	D2

and 12% (series D). In the remainder of the article, W_{ac} is the value taken into account for all calculations.

For each concrete (C1, D1, . . .), specimens (11 cm × 22 cm cylinders) were subjected to two different curing regimens.

Cure 1: Half the specimens was sealed and cured under controlled laboratory conditions (20°C) for 1 day.

Cure 2: The other half of specimens was sealed and cured under simulated conditions of hot weather in order to consider a time elapse between placing and transporting the specimens to the laboratory (cure 2): 35°C during the first 5 hours after casting, next progressive decrease in temperature down to 25°C until 24 hours after mixing.

At 24 hours, all the specimens were stored in a water tank at 20°C until the time of the tests.

Two Ways for Evaluating the 28-Day Degree of Hydration

Chemically Bound Water

Samples are taken from the core of 28-day specimens tested in compression and ground. A quartering is used in order to obtain representative specimens of the concrete composition. The amount of the chemically bound water is determined by the mass loss of the concrete specimens on heating from 105°C to 1000°C. The loss on ignition of volatile substances included in all the constituents are also taken into account. The 28-day degree of hydration α_{28w} is the ratio of the measured 28-day chemically bound water EL_{28} to that corresponding to 100% of hydration EL_∞:

$$\alpha_{28w} = \frac{EL_{28}}{EL_\infty}.$$

Referring to works of Powers and Brownyard [13], EL_∞ is considered to be equal to 25% per weight of anhydrous cement when OPC is used. For each concrete, α_{28w} is a mean value derived from three measurements of EL_{28}.

Image Analysis

Specimens are taken from the core of slices sawn out from the middle of concrete cylinders. They are resin-impregnated and dry-polished with silicon carbide grits down to 4 μm. The polishing is then finished with a 1-μm impregnated diamond cloth. This final grit size is recommended by Detwiler [14] in the case of concrete. Before observation, materials accumulated through the specimen surface are cleaned out ultrasonically in alcohol. Finally, carbon-coated surfaces are examined in the scanning electron microscope (SEM) using BSEI by inverse polarity so that the greater the mean atomic number of a solid phase of the sample, the darker this solid phase on the screen. In that condition, unhydrated clinker compounds appear black. A voltage of 15 kV and a working distance of 15 mm are used in this study. Each image obtained from the SEM is digitized in an hexagonal lattice into a 740 × 625 matrix of pixels with 256 gray levels.

The degree of hydration is calculated by counting on each image all the pixels identified as anhydrous phase. According to the stereology rules, the area fraction derived is equal to a volume fraction, assuming a homogeneous and isotropic distribution of the cement grains through a basic volume of cement paste in concrete. Hence, the degree of hydration based on image analysis α_{28IA} is written as:

$$\alpha_{28IA} = 1 - \frac{A_{28}}{\Gamma_0}$$

where A_{28} = area fraction of anhydrous remnant cement grains present in the cement paste of concrete at 28 days of age, and Γ_0 = initial volume fraction of cement grains present in the fresh paste of concrete.

For each sample, ten fields at 100× magnification are necessary so that the variation in the average A_{28} is approximately equal to 2.0%.

The image analysis procedure is based on the entropy maximization of the gray level histogram [15]. The entropy maximization leads to maximization of the contrasts between gray level categories in order to determine one or several critical thresholds in the gray level histogram. In this case, the method is applied to extract three gray level families in the gray level histogram of an image and so to distinguish two critical

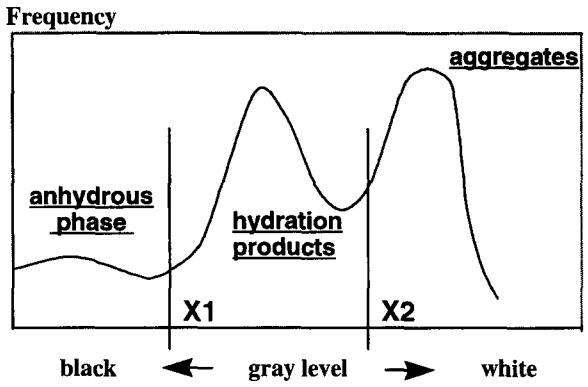

FIGURE 1. Gray level histogram.

thresholds X1 and X2 (Figure 1). The entropy H is written as:

$$H(X1, X2) = -\sum_{i=0(\text{black})}^{X1} Pi \ln Pi - \sum_{i=X1+1}^{X2} Pi \ln Pi - \sum_{i=X2+1}^{255\ (\text{white})} Pi \ln Pi$$

where Pi = probability that a pixel reaches the gray level i. These optimal thresholds are then found with a maximum probability so that the first gray level class is representative of the unhydrated compounds (behind X1), the second gray level category includes hydration products, and the third one, aggregates (beyond X2).

Five steps are necessary to perform an automated procedure.

1. *Filtering*. The contrast is enhanced between anhydrous materials and other phases present in the cement paste (Figures 2a and 2b).
2. *Binarization by the entropy maximization of the gray level histogram*. Two critical thresholds are extracted, which results in two binarized images corresponding to the recognition of anhydrous particles (Figure 2c) and aggregates (Figure 2d), respectively.
3. *Fine aggregate extraction* (Figure 2e). This step is principally composed of aggregate edge closing and aggregate hole closing. These operations induce a relative error of about 0.1%. Aggregate hole closing allows removal of inclusions whose gray levels are close to those of cement paste. In some cases, it is necessary to manually draw the perimeter of aggregates whose gray level values are almost equal to those of the cement paste (see the black-surrounded aggregates in Figure 2d). The corresponding relative error was evaluated to be <0.5%.
4. *Fine anhydrous phase extraction* (Figure 2f). Parts of unhydrated cement grains may be hidden by unremoved grits or plucked from the specimen surface. These artifacts are erased by hole closing.
5. *Rebuilding of the image* (Figure 2g).

Magnification at 100× was used in order to ensure a representative sampling, but the size of the remnant cement grains size detected was limited by the resolution (2.07 μm). To obtain a reasonable estimate for the anhydrous area of the whole sample, the same concrete area was examined either at 100× or 400× magnification. In this way, anhydrous areas ≤3.0 μm had to be neglected at 400× magnification to fit the results at 100× magnification. Consequently, it was found that A_{28} determined at 100× magnification has to be increased at least by 17%. Results given below are corrected accordingly.

28-Day Compressive Strength

The 28-day compressive strengths are given in Table 2. It clearly appears that: the compressive strengths are reduced when the curing temperature is increased; and in every case, the compressive strengths are reduced with the rise in initial temperatures inducing additions of water to maintain the slump.

Degree of Hydration

Figures 3 and 4 give the degrees of hydration and their evolution according to both methods, with their experimental scatter. In the case of image analysis, the scatter corresponds to 10 successive measures of A_{28} on two samples, respectively. Concerning the chemically bound water, it results from three measurements.

When evaluating the degree of hydration by means of the chemically bound water, it can be observed that increases in temperature of both the initial condition and curing induce higher values.

The same trends cannot be pointed out from image analysis. With regard to series C, the degree of hydration α_{28IA} decreases with the rise in the initial temperature, whatever the curing regimen may be. Concerning series D, there is an increase in α_{28IA} with the same rise in the initial temperature without significant differences induced by the curing regimen.

When analyzing α_{28IA} values, it must be noticed that series D is more hydrated than series C. This can be explained by considering that cement grains are more dispersed in series D (w/c ratio = 0.73 to 0.85) than in series C (w/c ratio = 0.52 to 0.58) [16].

In Figure 5, values of α_{28IA} are plotted vs. α_{28w}. This diagram shows that image analysis generally leads to

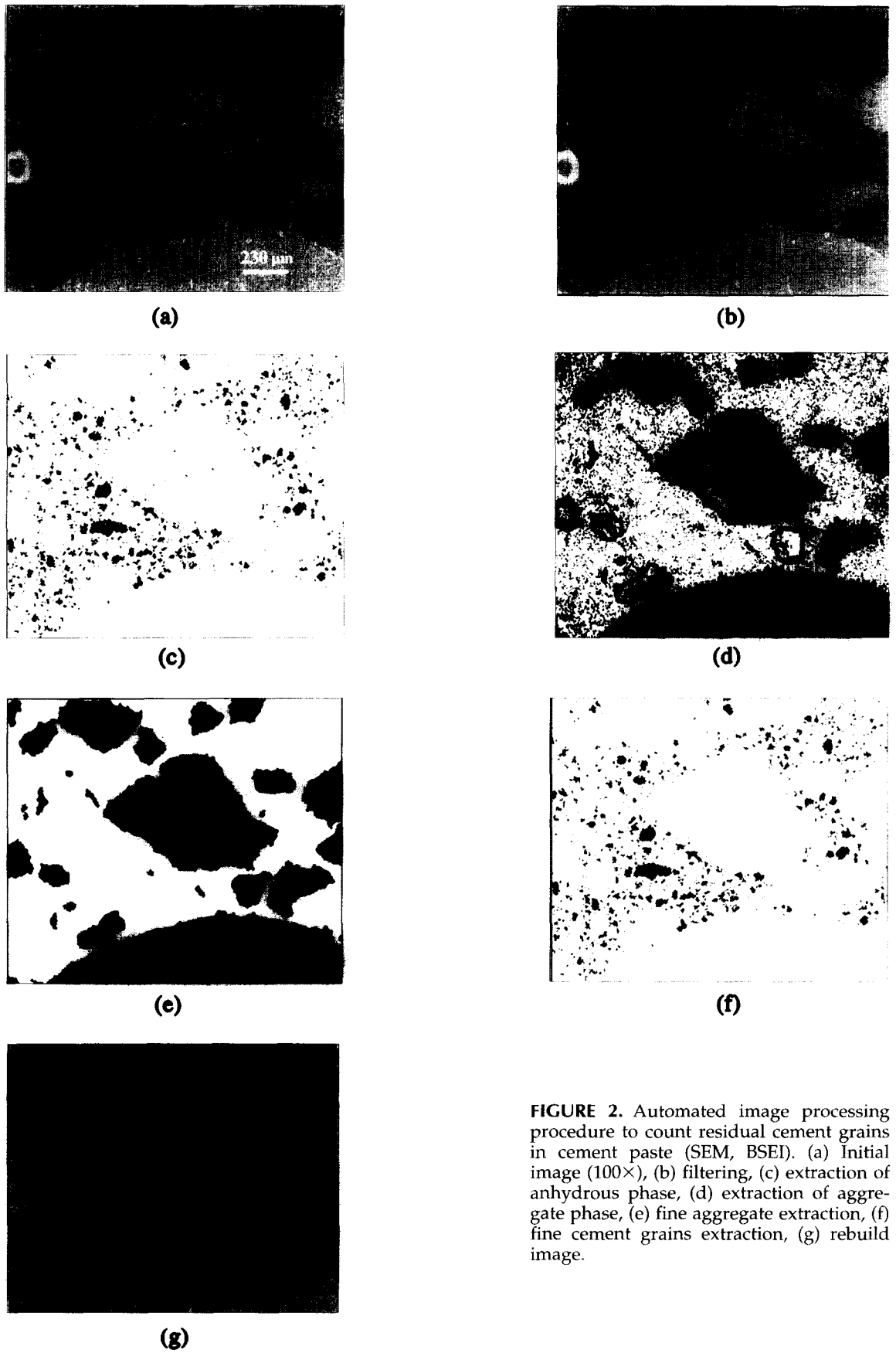

FIGURE 2. Automated image processing procedure to count residual cement grains in cement paste (SEM, BSEI). (a) Initial image (100×), (b) filtering, (c) extraction of anhydrous phase, (d) extraction of aggregate phase, (e) fine aggregate extraction, (f) fine cement grains extraction, (g) rebuild image.

TABLE 2 Compressive strength results

	Cure 1		Cure 2	
	Average* (MPa)	SD (MPa)	Average* (MPa)	SD (MPa)
C1	38.4	1.3	34.6	0.8
C2	34.5	0.2	32.1	0.6
D1	28.1	0.6	24.8	0.7
D2	23.0	0.4	22.1	0.6

Note: *Mean of six values.

higher values than those derived from bound water measurements. Two main causes can explain this scatter.

On the one hand, loss on ignition accounts for all the hydration products, in the bulk paste as well as in the interfacial zone. This is true provided there are no artifacts induced by the method. Unfortunately, up to 105°C, a part of EL_{28} is not taken into account because of the likely beginning of the dehydration of C–S–H, AFm, and AFt phases [17]. Moreover, EL_{∞} is a datum suitable for a previous study [13] and, consequently, an estimated value in the case of the cement used here.

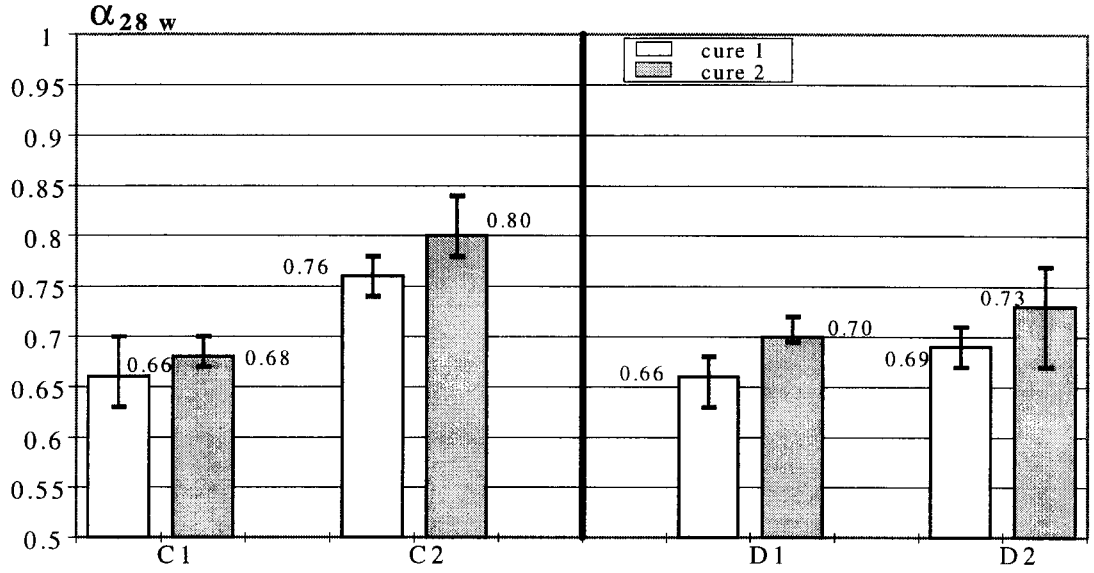

FIGURE 3. α_{28w} average and corresponding experimental scatter.

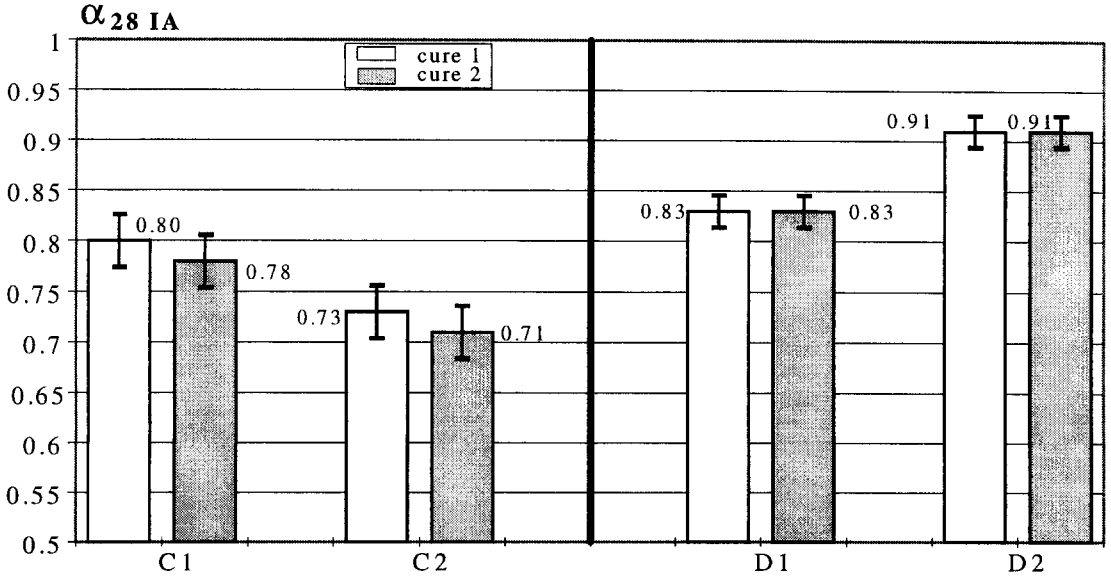

FIGURE 4. α_{28IA} average and corresponding experimental scatter.

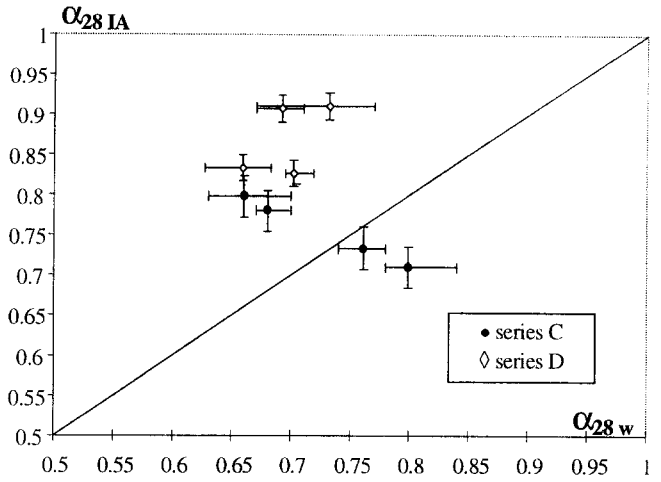

FIGURE 5. Comparison of α_{28IA} and α_{28w}.

On the other hand, using image analysis the hydration products are not discriminated, particularly those at the interfacial tranzition zone (ITZ), and the paste area is considered to be homogeneous. Therefore, a global picture of the paste is given. To be able to discriminate them, further developments are necessary to convert volume measurements into mass values and notably to account for porosity.

Nevertheless, even if both methods provide results that seem contradictory, α_{28} variations observed using each method give rise to the following statements.

- As drops in strength are not correlated with α_{28IA} variations, it may be concluded that the mechanical performances do not primarily depend on the bulk paste in the way it was observed.
- α_{28w} is found to be systematically raised when the strengths decrease. This cannot be attributed to an increase in the amount of the same hydration products. With regard to image analysis, such an evolution of α_{28w} according to the initial temperature conditions may be due only to the formation of different products or to the formation of different-shaped hydration products.

Besides hydration measurements, SEM and ESEM observations were carried out that support the last point [18]. They highlighted a presence of more-or-less oriented crystals of portlandite at the paste-aggregate interface with the increase in initial temperatures (both mixing and curing ones). It was also noticed on aggregate imprints that when concrete was subjected to a 35°C curing temperature (cure 2), there were developed crystallizations, such as interminglings of little ettringite rods and massive crystals of portlandite, resulting in an aerated texture and open microstructure of the paste. Therefore, modified conditions of temperature involve a drop in concrete strength as a result of a weakening of ITZ.

Conclusions

Two methods were used to evaluate the 28-day degree of hydration of concrete: image analysis on flat polished sections observed by SEM (α_{28IA}) and classical measurement of the chemically bound water (α_{28w}). The scope was to link the strength variations to the hydration state. For this purpose, two series of normal strength concrete were performed: (1) series C, 28-day nominal strength of 35 MPa; and (2) series D, 28-day nominal strength of 22 MPa.

For each series, differences of 28-day compressive strength were obtained by varying both initial and curing temperatures. Initial temperatures were either 20°C or 50°C by heating the constituents. In each case, concrete was subjected either to 20°C curing temperature for 24 hours or to 35°C for 5 hours with progressive decrease down to 25°C until 24 hours. The following conclusions were obtained:

1. Drops in 28-day compressive strength occur with the increase in either the initial temperature or curing temperature. Drops in strength are more pronounced when both initial and curing temperatures are raised.
2. α_{28w} increases with the rise in initial temperature conditions whereas α_{28IA} variations depend on the class of concrete. Moreover, α_{28IA} values of series D are greater than those of series C. This is explained by:
   - Smaller A_{28} values measured for series D,
   - Larger W/C ratios for series D, inducing an initial dispersed distribution of the clinker phase in the paste and of course Γ_0 values higher for series C than for series D.
3. α_{28IA} values are generally higher than α_{28w} ones. The two following points can at least clarify this difference.
   i. The chemically bound water EL_{28} is counted from 105°C to 1000°C; below 105°C, a part of the dehydration of C–S–H, AFm, and AFt phases is not taken into account. Besides this, the amount of chemically bound water corresponding to the limit of hydration is a datum based on previous studies and somewhat an arbitrary value with regard to any used cement.
   ii. α_{28IA} is derived directly from the ratio of the anhydrous volume to the paste one. Here the paste is considered as homogeneous without distinction between hydration products, partic-

ularly those at the ITZ. In order to discriminate them, it is necessary to convert both anhydrous and paste volumes into mass values.

4. α_{28IA} variations cannot explain the drops in strength. Therefore, these drops cannot be linked to changes in the paste in the way it was observed. But, with regard to the image analysis method, the evolution of α_{28w} reveals that the modified initial conditions of temperature involve the formation of either different hydration products or different-shaped hydration products. Such variations with the increase in initial temperatures are effectively observed at ITZ by SEM and ESEM.

Acknowledgments

The authors are grateful to Association Technique de l'Industrie des Liants Hydrauliques for supporting this research and to Dr. E. Ringot for help to develop the image analysis method.

References

1. ACI Committee 305. *J. Am. Concr. Inst.* **1991,** *88,* 417–436.
2. Mouret, M.; Bascoul, A.; Escadeillas, G. in *Proc. Mater. Res. Soc. Symp.*; Scrivener, K.L.; Young, J.F., eds. **1995,** 227–234.
3. Taplin, J.H. *J. Aus. Appl. Sci.* **1962,** *13,* 164–171.
4. Byfors, J. *CBI Research Report, No. 3:80*; Swedish Cement and Concrete Research Institute: Stockholm, 1980; pp 53–54.
5. Odler, I.; Gebauer, J. *Zement-kalk gips.* **1966,** *55,* 276–281.
6. Scrivener, K.L.; Pratt, P.L. In *Proc. 1st RILEM International Congress, Versailles;* **1987,** *1,* 61–68.
7. Bentz, D.P.; Jennings, H.M. In *Proc. 1st RILEM International Congress, Versailles;* **1987,** *1,* 49–56.
8. Lange, D.A. *Cem. Concr. Res.* **1994,** *24,* 841–853.
9. Diamond, S.; Leeman, M.E. In *Proc. Mater. Res. Soc. Symp.* **1994,** *370,* 217–226.
10. Chan, S.L. In *Proc. Mater. Res. Soc. Symp.* **1994,** *370,* 111–118.
11. Al-Hassani, Y.; Bascoul, A.; Ringot, E. In *Proc. Mater. Res. Soc. Symp.* **1994,** *370,* 43–48.
12. Elsen, J.; Lens, N.; Aarre, T.; Quenard, D.; Smolej, V. *Cem. Concr. Res.* **1995,** *25,* 827–834.
13. Powers, T.C.; Brownyard, T.L. *Proc. ACI.* **1947,** *43,* 490.
14. Detwiler, R.J. In *2nd Canadian Symp. Cem. Concr.* **1991,** 84–92.
15. Coster, M.; Chermant, J.L. *Presses CNRS* **1989,** 390.
16. Granju, J.L.; Maso, J.C. *Cem. Concr. Res.* **1984,** *14,* 249–256.
17. Taylor, H.F.W. *Cement Chemistry;* Academic Press: London, 1990; p 220.
18. Mouret, M.; Bascoul, A.; Escadeillas, G. *Cem. Concr. Res.* (Submitted).